Digest Journal of Nanomaterials and Biostructures Vol. 14, No. 2, April - June 2019, p. 291 - 303

BIOSYNTHESIS OF COPPER OXIDE NANOPARTICLES USING THE PREFORMED BIOMASS OF ASPERGILLUS FUMIGATUS AND THEIR ANTIBACTERIAL AND PHOTOCATALYTIC ACTIVITIES

M. GHAREIB[a,*], W. ABDALLAH[a], M. ABU TAHON[a], A. TALLIMA[b]
[a]*Department of Biological and Geological Sciences, Faculty of Education, Ain Shams University, Roxy 11757, Cairo, Egypt*
[b]*Ministry of Education, Egypt*

Copper oxide nanoparticles (CuO NPs) were biosynthesized in this work using the preformed mycelium of *Aspergillus fumigatus*. They had amaximum absorption with sharp peak at 335 nm. On examination with high resolution transmission electron microscope (HR-TEM), the NPs were found spherical uniformly distribution with mean size of 6 nm. A clear edge was detected around the CuO NP when magnified in a preliminary indication of their crystalline nature that proved by X-ray diffraction (XRD) analysis. They retained full stability for at least six months on storage at 4^{o}C. Its zeta potential was found to be -28.2 mv. The antibacterial activity of these NPs was proved against two important human pathogens i.e. *Staphylococcus aureus* and *Klebsiella pneumonia*. Also, they succeeded in degradation of 97% methylene blue (MB) dye in direct sunlight after 200 min.

(Received January 20, 2019; Accepted April 6, 2019)

Keywords: Copper oxide, Nanoparticles, Biosynthesis, *A. fumigatus*, Antibacterial, photocatalysis

1. Introduction

With the beginning of the 21*st* century, nanobiotechnology entered the scientific spot-light as a discipline of manufacturing and applications of nanotechnology. Nanoparticles (NPs) are being the fundamental building blocks of this technology. Their small dimensions and high surface area to volume enable them to exhibit novel chemical and physical properties and consequently can be used in novel applications. Most research works in the field of NPs biosynthesis has been focused on silver and gold NPs. However other metal NPs have begun to draw the attention of researchers in the last years. Of these, copper NPs (CuNPs) have received some attention. The few papers in the literature on synthesis of CuNPs have been devoted to synthesize them in their oxide (CuO NPs or Cu_2O NPs) forms [1]. Cupric oxide (CuO) is a transition metal semiconducting material of *p*-type with a narrow band gap of 1.2-1.7 eV corresponds to visible light [2,3]. It has unique optical, electrical and magnetic properties and used for various applications, such as the development of super-capacitors, near-infrared filters, in magnetic storage media, sensors, catalysis, semiconductors, etc. [4]. CuO NPs are routinely produced through physical, chemical and biological methods. Quality of the NPs produced from the physical methods is found less as compared to those produced by the chemical methods. Usually the physical methods require costly vacuum systems to prepare NPs [5]. On the other hand, there are some limitations of using the chemical methods for synthesis of different NPs due to their use of toxic solvents, generation of harmful by-products [6] and absorption of toxic chemicals on the NPs surfaces [7] consequently can lead to undesirable effects when used for medical purposes. Biological techniques for biosynthesis of CuO NPs using plant extracts or various microorganisms are now described due to their high-yield, low cost, nontoxic, and environmentally benign procedures. Concerning the use of different microorganisms in this regard, there are only few reports compared to the great number for other metal NPs. A number of investigators used algae [8] and bacteria [1,9,10] as

*Corresponding author: mohaghareib@yahoo.com

tools for the green biosynthesis of CuO NPs. Among the biological systems used for the biosynthesis of NPs fungi have gained little attention. Fungi are simple to deal with in the laboratory and secrete large amounts of enzymes [11]. However, very few number of research works was recorded on the mycosynthesis of CuO NPs. A biological process for the formation of CuO NPs from copper sulfate ($CuSO_4$) using three different species of *Penicillium i.e. P. aurantiogriseum*, *P. citrinum* and *P. waksmanii* was reported [12]. Applicability of the white-rot fungus *Stereum hirsutum* for use in the biosynthesis of CuO NPs was also confirmed [11]. CuO NPs have received a lot of attention in a wide range of applications due to their unique properties and low cost preparation. The biomedical fields are the most important of their applications either directly by utilization of their antimicrobial properties or indirectly by lowering the toxicity of the wastewaters. Copper is well known as an essential element for living organisms making it suitable for biomedical applications [13]. The antibacterial activity of NPs has been studied largely with human pathogenic bacteria, mainly *Escherichia coli* and *Staphylococcus aureus*. In contrast to silver and gold NPs, those have been studied extensively for antibacterial application, the reports on the CuO NPs are relatively few [8,10,14]. The main current application of CuO NPs as antimicrobial agents is their use in hospitals [15]. Synthetic dyes used in many industries are of the main pollutants in wastewaters. These hazardous are non-biodegradable [16] and cannot be easily removed causing serious problems for humans and the environment. So, there is an urgent need to minimize their damaging effect. Several conventional biological [17,18], chemical [19] and physical [20] methods have been used for treatment of these pollutants. The previous traditional methods are not convenient because they transfer the pollutant from one phase to another [21] instead of the complete mineralization. With this drawback, the advanced oxidation processes (AOPs) have been suggested [22]. This clean technology has been successfully applied to attack the pollutants by generation of highly reactive radicals [23]. The AOPs are subdivided to homogeneous and heterogeneous, on the basis whether the process is carried out in a single phase or use semiconductor catalysts to carry out the degradation of organic pollutants [23]. Disadvantage of the homogeneous processes is their high cost and the arising of secondary pollution due to the use of excessive chemical**s.** On the other hand, the operating coasts of the heterogeneous photocatalysis processes are low. In addition, they worked under ambient conditions and mostly resulted in complete mineralization without secondary pollution [24]. Titanium dioxide (TiO_2) is the most investigated heterogeneous photocatalyst for degradation of a wide range of organic contaminants [21]. This is attributed to their efficiency, stability, non-toxicity and low cost. Other heterogeneous photocatalyst semiconductors like ZnO are investigated as catalytic agents for biodegradation of some dyes used in various industries [25,26]. Due to their high stability, low costs and nil toxicity, CuO NPs from different sources were also utilized as heterogeneous catalysts for dye biodegradation [27,28]. This work was devoted for biosynthesis of CuO NPs from a fungus not recorded in this regard before. Characterization of the produced NPs and their applications as antibacterial and photocatalytic agents were also ascertained.

2. Experimental

2.1. Chemicals and Glass wares

All chemical used in this work were of analytical grade. The reagent solutions were made with deionized water. The glass wares were washed with aqua regia (3:1 HCl-HNO3) and then thoroughly rinsed with deionized water to remove any metal contaminant.

2.2. Organism and cultivation

Aspergillus fumigatus Fresenius AUMC 13024 used in the work had been isolated from soil sample collected from Giza Governorate, Egypt and identified by Assiut University Mycological center (AUMC) where it is deposited with its accession number. It was selected in a preliminary screening program to access potentiality of the available fungi on the biosynthesis of CuO NPs. It was routinely grown on Czapek's- agar medium at 30^{o}C and sub-cultured whenever required. The fungus was grown in 250 ml Erlenmeyer flasks containing 50 ml of Czapek's-Dox broth having the following composition (g/100 ml)**:** Sucrose, 3; $NaNO_3$, 0.2; KH_2PO_4, 0.1; KCl,

0.05; $MgSO_4.7H_2O$, 0.05 and $FeSO_4.5H_2O$, 0.001. After sterilization, the flasks left to cool, initial pH of the fermentation medium was adjusted to pH 6 and inoculated with one ml of spore suspension (-10^6 conidia) obtained from 7-day-old culture. The cultures were incubated on rotary shaker adjusted to 150 rpm at 30°C for 72 h. By the end of the incubation period, the biomass was separated from the culture supernatant by filtration through Whatman filter paper No.1.

2.3. Biosynthesis of CuO NPs

The fungal biomass was washed extensively with deionized water to remove all possible components of the fermentation medium. Typically 10 g of biomass (fresh weight) was directly brought in contact with 90 ml of 1 mM of copper nitrate ($Cu(NO_3)_2.3H_2O$), kept on the rotary shaker at 30^{o}C and agitated at a velocity of 150 rpm for 60 h in the dark. Both positive (biomass in deionized water and negative (1mM $Cu(NO_3)_2.3H_2O$) controls were run along with the experimental flasks.

2.4. Characterization of the biosynthesized CuONPs

2.4.1. Visual observation and UV-Visible spectroscopy

The biosynthesized CuO NPs solution was routinely monitored by visual observation. Change in the colloidal solution towards green (or greenish) color was taken as preliminary sign of CuO NPs formation. To confirm the formation of CuO NPs, the UV-Vis spectrum of the reaction medium showing a change in color was monitored after filtration through 0.22 µm membrane filter (Millex-GS, Millipore, Madrid, Spain). Absorption measurements were carried out at wavelengths from 200 to 800 nm using a double beam spectrophotometer (Metash UV-Vis, model UV-8500) at a resolution of 1 nm. UV-Vis analysis was weekly carried out for six months to check NPs stability.

To get rid of any uncoordinated biological molecules, the solution containing the biosynthesized NPs was then centrifugation at 17000 rpm for 15 min and the settled CuO NPs were washed several times with deionized water. The NPs either air dried or re-suspended in deionized water by ultrasonication (Chem Tec Ultrasonic Processor UP-500, SN: UH005-0076) and used in further characterization. The centrifuging and re-dispersing processes were repeated three times.

2.4.2. Fourier Transform Infrared (FTIR) Spectroscopy

The dried NPs were used in this analysis. FTIR spectra were obtained using Berkin-Elmer 293 spectrometer. KBr discs were used as calibrant and all measurements were carried out in the range of 400–4000 cm^{-1} at a resolution of 4 cm^{-1}.

2.4.3. High Resolution-Transmission Electron Microscopy (HR-TEM)

The morphology and size of CuO NPs were performed in central lab of national research center (NRC), Dokki, Giza, Egypt. For this purpose, an aliquot of an aqueous suspension of CuO NPs was transferred onto a carbon coated copper grid. Samples were dried and kept under vacuum in desiccators before loading them onto a specimen holder. The grid was then scanned using a Jeol JEM-2100 (Made in Japan Model Year 2000) operated at a voltage of 200 kV.

2.4.4. Selected area electron diffraction (SAED)

SAED pattern for NPs is a crystallographic experimental technique that can be performed inside a TEM. This analysis requires a very thin sectioned specimen nearly 100 nm and a high energy electron volt (100-400 K.ev), so in this case electrons will act as wave not particle when interacting with analyzed material. The atoms in substrate will act as a grating making diffraction to falling electrons, so the diffraction pattern appears as a bright spot [29].

2.4.5. Zeta potential measurement

Zeta potential of CuO NPs was evaluated in nanomedicine and tissue engineering lab of NRC using a Malvern Zetasizer Nanoseries Nano ZS (Malvern Instruments Ltd, Malvern, UK). Data obtained were analyzed using Zetasizer software.

2.4.6. X-ray diffraction (XRD)

The XRD analysis was conducted on XPERT-PRO-PANalytical Powder Diffractometer (Netherland) using monochromatic Cu K α radiation (θ = 1.5406 Å) operating at a voltage of at 45 kV and a current of 30 mA at room temperature. The intensity data were collected over a 2θ range of 4.01°–79.99°.

2.4.7. Energy dispersive X-rays (EDX)

Samples were prepared on a copper substrate by drop coating of CuO NPs. Elemental analysis on single particles was carried out using Thermo Noran EDS attachment equipped with TEM.

2.5. Antimicrobial activity of the produced CuO NPs

2.5.1. Determination of minimal inhibitory concentration (MIC)

The micro dilution method in culture broth **w**as used for determination of MIC. Different concentrations of CuO NPs (10-100µg/ml) were prepared using sterilized distilled water and added to conical flasks of 50 ml capacity each contain 10 ml of sterilized Mueller Hinton broth of the following composition (g/100 ml): Casein hydrolysate, 1.75; beef extract, 0.3 and starch, 1.5. One flask devoid of the NPs was used as negative control and other flask devoid of the inoculum was used as a positive control. All flasks were inoculated with approximately 10^7 colony forming units (cfu)/ml of actively dividing bacterial cells. All experimental flasks were incubated on rotary shaker adjusted at 150 rpm and 37^{o}C for 24 h. At the end of the incubation period, absorbency value of OD 600 nm was determined.

2.5.2. Effect of NPs on membrane leakage

The test bacterial cultures were grown with shaking at 150 rpm on Mueller Hinton broth for 24 h at 37^{o}C then centrifuged and the supernatants were discarded. To detect the leakage of bio-molecules through membrane, different volumes of CuO NPs were so as to reach final test concentration (10-100µg/ml), and the test bacterial cells (5 ml) were adjusted to 10^9 cfu/ml. Control experiments were conducted without NPs. All cultures were incubated at 37^{o}C with shaking at 150 rpm for different contact time (1, 3 and 6 h) then centrifuged at 6000 rpm for 15 min and the concentrations of proteins, reducing sugars and nucleic acids were determined as soon as possible in the supernatant. Proteins by the procedure of Bradford [30**]**, reducing sugars by the 2,4-dinitrosalysilic reagent [31] and nucleic acids by measuring the absorbance at 260 nm using UV–Vis spectrophotometer [32]. All estimations were carried out in triplicates for reproducibility. The leakage of each component in the treated bacterial suspensions was expressed as percentage of its concentration in the control untreated bacterial suspensions.

2.6. Photodegradative activity of CuO NPs

Photocatalytic activity and degradability of CuO NPs was evaluated by monitoring the degradation of methylene blue (MB) and measuring its maximum absorption under sunlight irradiation. For this assay, 10 mg of synthesized CuO NPs was dispersed in one liter of distilled water (10µg/ml) in a beaker and ultrasonicated. Ten mg of the dye solution was added to the NPs solution (10-100µg/ml) and allowed to stir in the dark for 30 min until adsorption-desorption equilibrium was established. A dye solution with NPs was then placed under the exposure of natural summer sunlight irradiation for different time intervals between 11 am to 3 pm where fluctuation in the solar intensity is at its minimum [26]. At regular time intervals (every 20 min), aliquot of dye sample was withdrawn and centrifuged at 6000 rpm for 10 min to separate CuO NPs from the degraded dye solution by preventing the dispersion of NPs. The sample was then subjected to UV-Vis spectrophotometric analysis in the range of 300 to 800 nm. The maximum wavelength of MB is known to be 657nm. Control solution of MB was prepared and kept under the same conditions for comparing any change in color of the dye solution. Degradation percentage of dye solution was calculated from the following equation:

$$\text{Degradation percentage} = [A0 - At] / A0 \times 100\ \%$$

Where:

A0 = initial absorbance of dye solution before expose to sunlight

A*t* = absorbance of dye solution at different time intervals, t

2.7. Statistical analysis

The obtained data were statistically manipulated according to the mathematical principles described by Glantz [33]. The data expressed as mean along with the standard deviation (±), T-score and probability (P) values of three replicates of the investigated factors were computed. The results were considered highly significant (HS), significant (S) or non-significant (NS) where $p \leq 0.01$, ≤ 0.05 or > 0.05, respectively.

3. Results and discussion

Search for new antibacterial and photocatalytic agents with reasonable efficiency is the prime interest of some investigators in the last years. Synthesis, characterization and application of the semiconductor NPs particularly CuO NPs is a matter of research in this point. Most works were done using plant leaf extracts [34,35]. Few reports were reported on utilization of microorganisms especially fungi.

3.1. Biosynthesis of CuO NPs using *Aspergillus fumigatus*

The CuO NPs was produced in this work using the preformed biomass of the locally isolated fungus *A. fumigatus* that selected in a preliminary screening of some fungi to test their potentialities for the determined aims. After growth on Czapek's broth in submerged culture for 72 h, the washed biomass was added to 1mM $Cu(NO_3)_2.3H_2O$ solution and incubated on rotary shaker at 150 rpm for 60 h at 30^{o}C in the dark. The change of color from light blue to light green or greenish was a preliminary sign of CuO NPs biosynthesis at the time that no change in colors of both positive and negative controls. The change in color of the reaction mixture was attributed to specific surface plasmon resonance phenomenon that occurs in response to the collective oscillations of the conduction electrons confined to the NPs. The color intensity as well as the UV-Vis absorption spectrum of the produced CuO NPs had been presented in Fig. 1. A sharp peak with maximum absorption at 335 nm was recorded. Most recorded absorption spectra for CuO NPs from other sources show broad absorption peaks. They were observed at around 365 nm for NPs from the bacterium *E. coli* [9] and at 310 nm using *Eichhornia crassipes* [34] or 360 using *Ixora coccinea* [35] leaf extracts. The results showed that the filamentous fungi including the experimented fungus may have the ability to produce CuO NPs with good characteristics but it need some efforts to detect their hidden potentiality. Biosynthesis of CuO NPs using *A. fumigatus* that recorded in this respect for the first time is a step in this direction to consolidate the few previous findings in this area.

Different reaction conditions affecting the biosynthesis process was investigated in a preliminary study to maximize the yield obtained from this CuO NPs. The best favorable conditions were pH 6, 30^{o}C, in presence of 1mM $Cu(NO_3)_2.3H_2O$ after 60 h of shaking in the dark at 150 rpm.

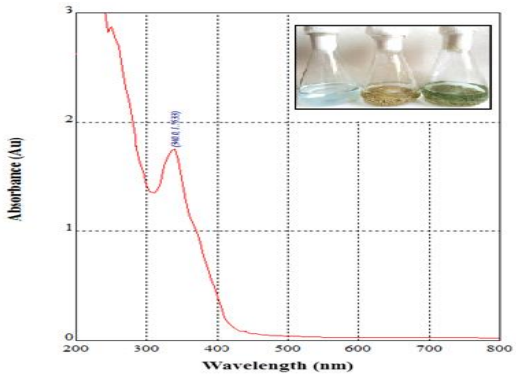

Fig. 1. UV-Vis absorption spectrum of CuO NPs formed using biomass of A. fumigates. Inset shows color change after incubating the biomass in 1mM copper nitrate (Right), in comparison with the biomass in double distilled water as positive (Middle) and copper nitrate alone as negative (Left) controls.

3.2. Characterization of the biosynthesized CuO NPs

Morphology and size of the biosynthesized CuO NPs were analyzed using HR-TEM. The micrograph (Fig. 2a) showed that the NPs are spherical and uniformly distributed. They had clear edges of crystal and lattice structure observed in HR-TEM micrograph (Fig. 2b) suggesting the crystalline nature of CuO NPs [36]. SAED of CuO NPs synthesized by the biomass of *A. fumigates* is presented in Fig. 2c.

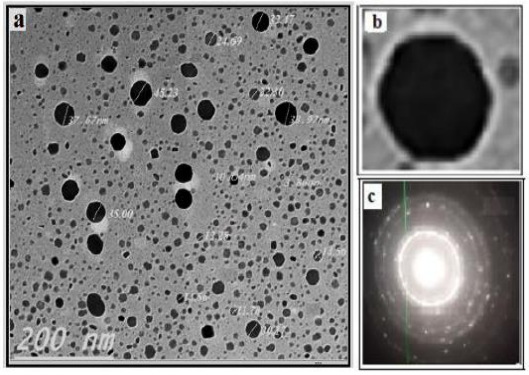

Fig. 2. HR-TEM micrographs of CuO NPs biosynthesized using A. fumigatus preformed biomass from $Cu(NO_3)_2$ 3.H_2O. (a) Showing spherical uniformly distributed NPs (b) Outlines of single magnified NP and (c) SAED pattern recorded for one NP.

The micrograph reveals the diffraction rings as lighted spots on the dark field. The circular rings, which can be indexed to the reflections from planes correspond to face-centered cubic (fcc) Cu and reveal the high crystalline nature of the biosynthesized NPs. Size distribution from TEM analysis (fig. 3) revealed that the produced NPs exhibit variation in size ranged up to 48 nm. The particle possess an average size of 8 nm representing 40.9% of the total count.

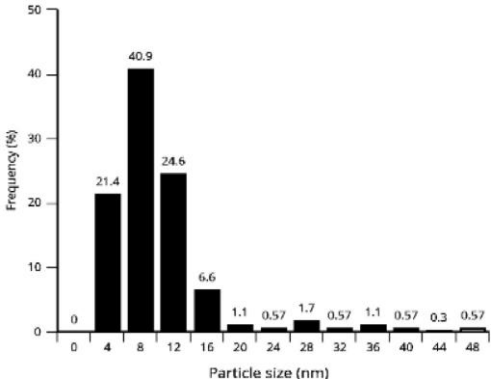

Fig. 3. Particle size distribution of CuO NPs from TEM analysis.

The XRD pattern of the biosynthesized CuO NPs is presented in fig. 4. The XRD pattern showed the diffraction peaks at degree 2θ = 32.8, 35.1, 38.6, 48.7, 53.2, 58.0, 61.5, 66.6, 68.3, 72.6 and 75.5 characteristic to indexing planes (110), (111), (111), (202), (020), (202), (113), (022), (220), (312) and (203), respectively. This agrees with the values reported for CuO NPs (JCPD file number 45-0937). The sharp and narrow diffraction peaks indicated high crystalline structure nature and phase purity of NPs.

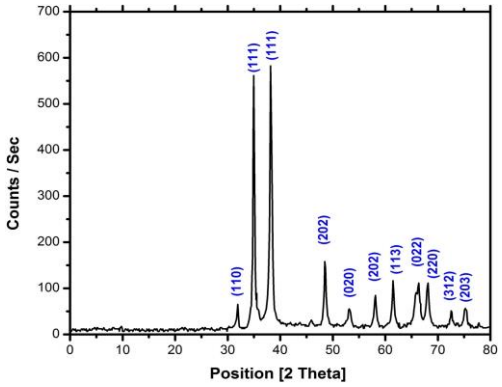

Fig. 4. XRD pattern of CuO NPs biosynthesized using biomass of A. fumigatus.

The FTIR spectroscopy was carried out to indicate the possible involvement of various functional groups or biomolecules in the formation and stabilization of CuO NPs. The technique is a powerful tool for identifying types of chemical bonds in a molecule by producing an IR spectrum that is like a molecular fingerprint. The FTIR spectrum of CuO NPs biosynthesized by *A. fumigatus* biomass was obtained in the wavelength range between 400 and 4000 cm^{-1} (Fig. 5). The broad intense absorption band at 3438.46 cm^{-1} corresponds to the hydroxyl (OH) functional group. Such group indicates the presence of polyphenols in the analyzed sample [37]. The band appeared at 2925.48 cm^{-1} represents the C–H stretching of aromatic compound of phenol group [37]. The characteristic bands recorded at 1643.05 cm^{-1} and 1546.63 cm^{-1} were those of the bending vibrations of amide-I and amide-II [38]. Amides I and II are the major bands in the protein IR spectrum and this suggested that proteins are interacted with the biosynthesized CuO NPs [2]. The band detected at 2856.06 cm^{-1} was described as C-H stretching corresponding to aromatic mode arises from aromatic amino acid [39**]**. The distinct bands found at 2373.94 cm^{-1}, 1430.92 and 1243, 86 cm^{-1} indicate the presence of –COO stretching [40**]** and $–CH_3$ bending bonds [41] and C-C stretching vibration of alkanes (38), respectively. Other distinct peaks recorded at 1313.29 cm^{-1} indicate the presence of C-N stretching vibration of the aromatic amines [42]. The band observed

at 1039.44 cm^{-1} confirms the presence of sulfur-containing amino acids in proteins of *A. fumigatus* [43]. Such proteins are known to act as an antioxidant under oxidative stress conditions [44]. Moreover, presence of the band at 771.38 cm^{-1} was assigned to aromatic groups [45]. Finally, the absorption peaks in the range of 692.32 cm^{-1} to 428.12 cm^{-1} reveal the vibrational modes of CuO [34, 40**]**. The previous findings confirm the presence of many chemical groups of different biomolecules attached to the NPs surface play different roles in biosynthesis, stabilization and functions of the investigated NPs.

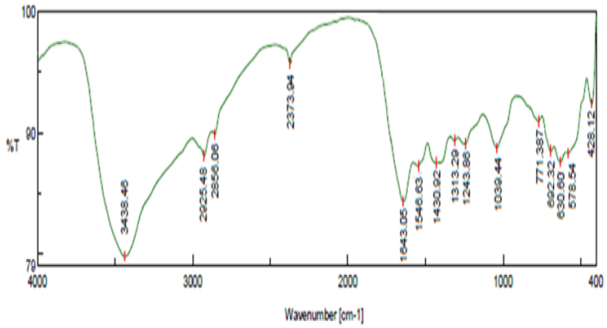

Fig. 5. FTIR spectrum of CuO NPs biosynthesized using biomass of A. fumigatus

The CuO NPs produced in this work was found stable for at least six months on storage at 4^{o}C where the absorption band did not change and there was no any sign of NPs agglomeration over this period. The presence of proteins and other chemical compounds correlated or bounded to the NPs surfaces as shown in the FTIR pattern can in part explain this stability. Zeta potential measurement of the biosynthesized NPs is shown in Fig. 6. Value of the surface charge was calculated to be -28.2 mV. The negative value cause repulsion among the NPs keeping their stability and prevents their aggregation.

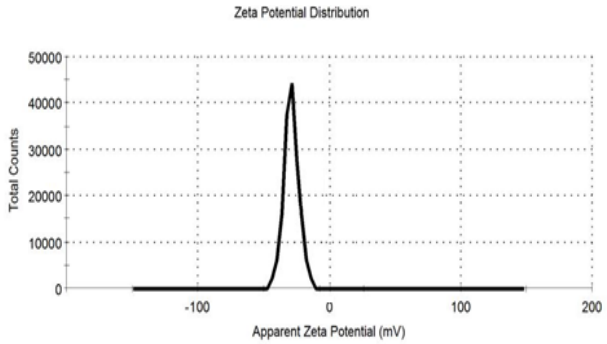

Fig. 6. Zeta potential measurements of the biosynthesized NPs.

EDX spectroscopy is applied to quantify the elemental composition of the biosynthesized CuO NPs. The EDX pattern of the produced NPs (Fig. 7) revealed the presence of the signal characteristic of copper (Cu) and oxygen (O) elements. The weights percent of copper and oxide calculated from EDX were O: 12.09 weight % and Cu: 87.91 weight %, respectively. The peak around 0.5 keV belongs to the binding energy of oxygen (O K), while peaks located at binding energies of 1.0, 8.1 and 9.0 keV correspond to, Cu L, Cu Ka and CuKβ, respectively. No signals arising from any impurity have been detected in the EDX spectrum.

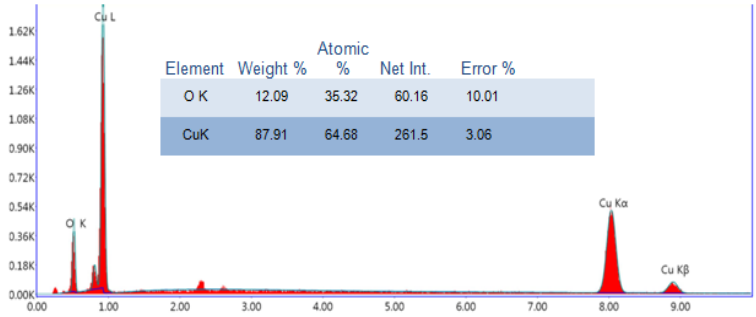

Fig. 7. EDX pattern of CuO NPs from A. fumigatus biomass

3.4. Antibacterial activity of the biosynthesized CuO NPs

The unique physiochemical properties of NPs make them possible to be used in different fields of application. The biomedical field is one of the most important due to its direct contact with human's healthcare. Resistance of human bacterial pathogens is a big challenge in the biomedicine. There is an increasing prevalence of pathogenic multidrug-resistant (MDR) bacteria globally. MDR bacteria are those resistant to many different antibiotics. They are difficult to treat so an urgent need for alternative ways to enhance potentialities of the antibiotics or search for new efficient antibacterial materials. The progress in nanotechnology applications led to introduction of NPs as alternative to the conventional antibiotics due to their high surface-area-to-volume ratio and the unique physicochemical properties. Most investigators used either silver and/or gold NPs in this respect. Other metal and metal oxide NPs are recently investigated and found suitable to certain extent.

Antimicrobial activity of the mycologically green synthesized CuO NPs against two human bacterial pathogens i.e. the gram positive *Staphylococcus aureus* ATCC 8538 and the gram negative *Klebsiella pnemonia* ATCC 27736 was studied in term of the MIC which is the lowest concentration of CuO NPs that did not allow any visible growth on the basis of turbidity after 24 h of incubation. The results (Table 1) demonstrate a fluctuation effect of the NPs on the test bacteria due to difference of cell wall composition but the effect was more pronounced against the Gram +ve bacteria.

Table 1. Antibacterial activity of different concentrations of the biosynthesized CuO NPs against two human bacterial pathogens and determination of their MIC

CuO NPs (µg/ml)	Growth inhibition (%)	
	Gram +ve	Gram -ve
	S. aureus	*K. pneumonia*
0	0	0
10	10.9± 0.13 ^{HS}	10.3± 0.09 ^{HS}
20	26.3± 0.29 ^{HS}	23.6± 0.11 ^{HS}
30	48.4± 0.22 ^{HS}	37.9± 0.16 ^{HS}
40	81.3± 0.21 ^{S}	69.8± 0.32 ^{S}
50	100.0± 0.26●	90.0± 0.33 ^{NS}
60	-----	100.0 ± 0.16●

● *MIC to which the obtained data were statistically compared.*

The MIC was found to be 50 and 60 µg/ml for the previous pathogens, respectively. The antibacterial activity of CuO NPs was rendered to some reasons but their precise mechanism is yet to be fully understood. The small particle size of the NPs is an important factor in the antibacterial activity of the NPs due to their large surface area to volume ratio. The previous results of the FTIR revealed the presence of proteins and other biomolecules adsorbed to the surface of the biosynthesized CuO NPs that can augment their antimicrobial property [46]. The good

antibacterial activity of CuO NPs can be attributed to the generation of excess free radicals (FRs) and formation of oxidative stress [47].

Oxidative stress lead to damage of the bacterial cells by formation of pores and leakage of the intracellular components like sugars, proteins and nucleic acids. Leakage of these intracellular components was a clear indication for the bacterial cell wall damage owing to the presence of NPs that finally lead to cell death [46,47]. In this work, the test bacterial cells of 24 h age when contacted with the CuO NPs at their MIC showed leakage of the intracellular sugars, proteins and nucleic acids after different contact periods (Table 2). The reducing sugars were leaked early in comparison with the other two components. They were completely leaked from *S. aureus* and *K. pneumonia* after 3 and 6 h of contact with CuO NPs, respectively. More than 90% of the intracellular proteins and more than 80% of nucleic acids of their original contents were leaked after 6 h. It is of interest to note that the Gram +ve bacterium was more sensitive to the action of CuO NPs than the Gram –ve on.

3.2. Photocatalytic degradative effect of the biosynthesized CuO NPs

Effect of the generated FR did not limited to the antibacterial effect of the NPs but extended to the disposal of dyes used in many industries from the wastewater channels that cause a drastic problem since these pollutants are toxic and hard to biodegrade [16]. Although there are many conventional methods for dye removal from industrial wastewaters, they are not completely efficient but usually convert pollutants from one form to another [21].

Table 2. Leakage of intracellular components from the bacterial cells treated with their MIC of CuO NPs.

Components	Contact time (h)	Leakage (%)	
		Gram +ve	Gram -ve
		S. aureus	*K. pneumonia*
Reducing Sugars	1	64.6±0.09 ^{HS} (4.7±0.05)	56.6±0.19 ^{HS} (3.8±0.07)
	3	100.0±0.25 ^{HS} (12.0±0.20)	97.1±0.22 ^{S} (7.9±0.11)
	6	-- (13.9±0.18)	100.0±0.33 ^{HS} (11.2±0.09)
Proteins	1	42.4±0.22 ^{HS} (3.4±0.09)	37.7±0.31 ^{HS} (3.1±0.11)
	3	84.3±0.08 ^{HS} (3.6±0.06)	82.1±0.19 ^{HS} (3.2±0.11)
	6	96.0±0.43 ^{HS} (3.7±0.26)	93.0±0.25 ^{HS} (3.6±0.08)
Nucleic acids	*1*	*34.3±0.58* ^{NS} *(3.2±0.17)*	*29.5±0.13* ^{HS} *(2.9±0.03)*
	3	*77.8±0.20* ^{HS} *(4.9±0.31)*	*73.4±1.11* ^{NS} *(5.8±0.22)*
	6	*89.0±0.50* ^{HS} *(5.2±0.17)*	*84.0±0.73* ^{HS} *(6.7±0.14)*

In each case, the 1st line represents results of the treated samples and the results in parentheses represent their controls

The CuO NPs biosynthesized in this work was successfully used in the photodegradation of MB which is one of the predominant dyes in various industries under direct sunlight. Acute exposure to MB may cause tissue narcosis, heart stroke, jaundice, etc., in humans [48,49]. The degradation was detected visually by observing the gradual change in the color of the MB solution from blue to colorless (Fig. 8).

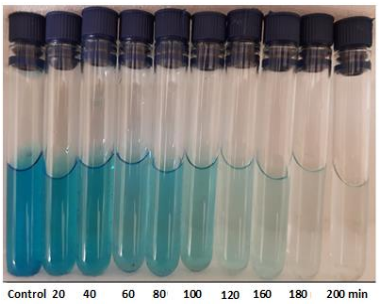

Fig. 8. Gradual change of MB color from blue to colorless.

The dye degradation (%) was calculated to be 97 % after 200 min as detected by the reduction of color intensity when evaluated at their absorption maximum i.e. 657 nm (Fig. 9). No change in coloration of the control treated in the same way. The previous results [27,28] accord with the results obtained in this work. Using this technique seems to be the most practical process for complete mineralization of these pollutants due to its low cost with no extreme conditions and nil toxicity. Three main components are involved in the degradation process: light, CuO NPs as a catalyst and oxygen. The catalyst is activated by the sun light to generate powerful oxidizing agents with the help of oxygen [23,24]. Due to the narrow band gap of CuO semiconductor which corresponds to visible light, the energy of sun appeared to be enough to excite the valence electrons to the conduction band, leading to the generation of electron-hole pairs [50]. Such technology depends upon formation of reactive hydroxyl radicals (OH^-) that reduce and decompose the organic dye [51]. The CuO NPs semiconductor photocatalyst speeds up the action of light by absorbing photon and production of electrons and holes [52].

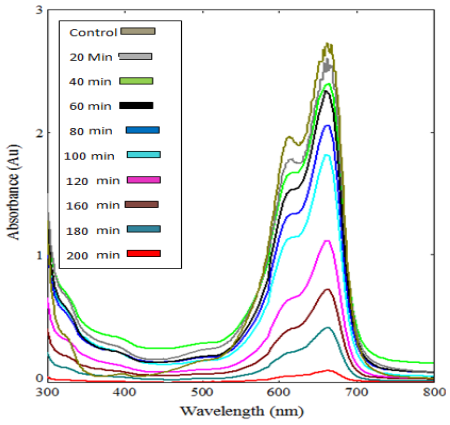

Fig. 9. UV-Vis spectra for photocatalytic degradation of MB by CuO NPs biosynthesized using A. fumigatus.

4. Conclusions

Biosynthesis of copper oxide nanoparticles by fungi is rarely investigated although their excellent fermentation potentiality. Out of twenty fungal species screened as possible producers for these nanoparticles *Aspergillus fumigatus* was recorded for the first time in this work as suitable producer of the copper nanoparticles using its preformed mycelium. The biosynthesized nanoparticles were spherical in shape with average size of 8 nm and characterized by their stability and crystalline structure. They found to have good antibacterial and photocatalytic activities.

References

[1] S. S. Hasan, S. Singh, R.Y. Parikh, M. S. Dharne, M. S. Patole, B. L. Prasad, Y. S. Shouche, J. Nanosci. Nanotechnol. **8**(6), 3191 (2008).
[2] M. George, S.J. Britto, European J. Biomed. Pharma. Sci. **1**(2), 199 (2014).
[3] N. R. Dhineshbabu, V. Rajendran, N. Nithyavathy, R. Vetumperumal, R, Appl. Nanosci. **6**, 933 (2016).
[4] S. Dagher, Y. Haik, A. I. Ayesh, N. Tit, J. Lumin. **151**, 149 (2014).
[5] A. Umber, S. Naveed, N. Ramzan, NANO: Brief Reports and Reviews **7**(5), 1230005, (2012).
[6] K. N. Thakkar, S. S. Mhatre, R. Y. Parikh, Nanomed. Nanotechnol. Biol. Med. **6**(2), 257 (2010).
[7] S. Gunalan, R. Sivaraj, R. Venckatesh, Spectrochim. Acta A: Mol. Biomol. Spectrosc. **97**, 1140 (2012).
[8] Y. Abboud, T. Saffaj, A. Chagraoui, A. El Bouari, K. Brouzi, O. Tanane, B. Ihssane, Appl. Nanosci. **4**, 571 (2013).
[9] H. R. Ghorbani, I. Fazeli, A. Asghar, Orient. J. Chem. **31**(1), 515 (2015).
[10] M. Taran, M. Rad, M. Alavi, Pharma. Sci. **23**, 198 (2017).
[11] D. Mandal, M. E. Bolander, D. Mukhopadhyay, G. Sarkar, P. Mukherjee, Appl. Microbiol. Biotechnol. **69**, 485 (2006).
[12] S. Honary, H. Barabadi, B. Ghara-El Fathabad, F. Naguib, Digest J. Nanomat. Bios. **7**(3), 999 (2012).
[13] O. Rubilar, M. Rai, G. Tortella, M. C. Diez, A. B. Seabra, N. Duran, Biotechnol. Lett. **35**(9), 1365 (2013).
[14] D. Das, B. C. Nath, P. Phukon, S. K. Douli, Colloids Surf. B. Biointerfac. **101**, 430 (2013).
[15] A. Lazary, I. Weinberg, J. J. Vatine, A. Jefidoff, R. Bardenstein, G. Borkow, N. Ohana, Int. J. Infect. Dis. **24**, 23 (2014).
[16] W. Jo, R. Tayade, Chinese J. Catal. **35**(11), 1781 (2014).
[17] G. McMullan, C. Meehan, A. Conneely, N. Kirby, T. Robinson, P. Nigam, I. M. Banat, R. Marchant, W.F. Smyth, Appl. Microbiol. Biotechnol. **56**, 81(2001).
[18] C. Pearce, J. Lloyd, J. Guthrie, Dyes and Pigments **58**, 179 (2003).
[19] A. Verma, R. Dash, P. Bhunia, J. Environ. Manag. **93**, 154 (2012).
[20] M. Marcucci, G. Nosenzo, G. Capannelli, I. Ciabatti, D. Corrieri, G. Ciardelli, Desalin. **138**, 75 (2001)
[21] F. Kazemi, Z. Mohamadnia, B. Kaboudin, Z. Karimi, J. Appl. Polum. Sci. **133**(19), 43386 (2016).
[22] Y. Deng, R. Zhao, Curr. Pollution Rep. **1**(3), 167 (2015).
[23] A. Ribeiro, O. Nunes, M. Pereira, A. Silva, Environ. Int. **75**, 33 (2015).
[24] M. Chong, B. Jin, C. Chow, C. Saint, Water Res. **44**, 2997 (2010).
[25] A. Zyoud, A. Zu'bi, M. H. S. Helal, D. DaeHoon Park, G. Guy Campet, H. S. Hilal, J. Environ. Heal. Sci. Eng. **13**, 46 (2015).
[26] H. C. Basavaraju, J. P. Shubha, Indian J. Adv. Chem. Sci. **S1** 56 (2016).
[27] H. A. Jassim, A. Khadhim, A. Al-Amiery, Int. J. Comput. Appl. Sci. **2**(2), 108 (2017).
[28] G. Manjari, S. Saran, T. Arun, A.V. B. Rao, S. P. Devipriya, J. Saudi Chem. Soc. **21**, 610 (2017).
[29] C. O. Ruud, C.S. Barrett, P. A. Russell, R. L. Clarck, Micron. **7**(1), 115 (1976).
[30] M. M. Bradford, Anal. Biochem. **72**, 248 (1976).
[31] G. L. Miller, Anal. Chem. **31**(3), 426 (1959).
[32] A. Álvarez-Ordónez, A. Carvajal, H. Arguello, F. J. Martínez-Lobo, G. Naharro, P. Rubio, J. Appl. Microbiol. **115**, 50 (2013).
[33] A. S. Glantz, "Primer biostatistics" McGraw Hill Inc. USA, 2 (1992).
[34] P. Vanathi, P. Rajiv, R. Sivaraj, Bull. Mat. Sci. **39**(5), 1165 (2016).
[35] S. M. Yedurkar, C. B. Maurya, P.A. Mahanwar, J. Mat. Environ. Sci. **8**(4), 1173 (2017).
[36] R. Raliya, J. C. Tarafdar, Agric. Res. **2**(1), 48 (2013).
[37] A-R Phull, Q. Abbas, A. Ali, H. Raza, S. J. kim, M. Zia, I. Haq, Future J. Pharma. Sci. **2**,

31 (2016).
[38] R. Cuevas, N. Durán, M. C. Diez, G. R. Tortella, O. Rubilar, J. Nanomat. 789089 (2015).
[39] R. Sanghi, P. Verma, Adv. Mat. Lett. **1**(3), 193 (2010).
[40] S. M. Dhoble, N. S. Kulkarni, Sch. Acad. J. Biosci. **4**(11), 1022 (2016).
[41] M. Rajarathinam, P. T. Kalaichelvan, Int. Res. J. Pharm. **4**(7), 68 (2013).
[42] S. C. G. K. Daniel, G. Vinothini, N. Subramanian, K. Nehru, M. Sivakumar, J. Nanopart. Res. **15**, 1319 (2013).
[43] R. Singh, V. D. Mendhulkar, J. Chem. Pharm. Res. **7**(6), 205 (2015).
[44] J. Moskovitz, Biochim. Biophys. Acta. **1703**(2), 213 (2005).
[45] S. J. P. Jacob, R. Bharathkumar, G. Ashwathram, World J. Pharm. Res. **3**, 3044 (2014).
[46] M. D. Balakumarana, R. Ramachandrana, P. Balashanmugama, D. J. Mukeshkumarb, P. T. Kalaichelvana, Microbiol. Res. **182**, 8 (2016).
[47] Y-G. Yuan, Q-L. Peng, S. Gurunathan, Int. J. Mol. Sci. **18**, 569 (2017).
[48] M. M. Nassar, Y. H. Magdy, Chem. Eng. J. **66**(3), 223 (1997).
[49] K. Vasanthkumar, V. Ramamurthi, S. J. Sivanesan, Colloid Interface Sci. **284**(1), 14 (2005).
[50] A. B. Gorospe, M. U. Herrera, J. Phys.: Conf. Ser. **817**, 012058 (2017).
[51] D. Suresh, P. C. Nethravathi, Udayabhanu, H. Rajanaika, H. Nagabhushana, S. C. Sharma, Mat. Sci. Semicond. Proc. **31** 446 (2015).
[52] J-M. Herrmann, Catal. Today **53**, 115 (1999).